PAPER

New fused conjugated molecules with fused thiophene and pyran units for organic electronic materials†

Daoliang Chen,[ab] Danlei Zhu,[ab] Gaobo Lin,[ab] Mingxu Du,[a] Dandan Shi,[ab] Qian Peng, [a] Lang Jiang, [a] Zitong Liu, [a] Guanxin Zhang[a] and Deqing Zhang [*ab]

Rigid and planar conjugated molecules have substantial significance due to their potential applications in organic electronics. Herein we report two highly fused ladder type conjugated molecules, **TTCTTC** and **TTTCTTTC**, with up to 10 fused rings in which the fused-thiophene rings are fused to the chromeno [6,5,4-*def*]chromene unit. Both molecules show high HOMO levels and accordingly they can be oxidized into their radical cations with absorptions extending to 1300 nm in the presence of trifluoroacetic acid. Thin films of **TTCTTC** and **TTTCTTTC** exhibit p-type semiconductor properties with hole mobilities up to 0.39 cm^2 V^{-1} s^{-1}. Moreover, **TTCTTC** shows a high fluorescence quantum yield of up to 16.5% in the solid state.

Introduction

Fused conjugated molecules such as arene analogues with heteroatoms including sulfur and nitrogen have been intensively studied,[1] with the aim of improving the stabilities of arene-based conjugated molecules, tune their HOMO/LUMO energies,[2] modulate the intermolecular interactions and thus improve their semiconducting properties.[3] In comparison, examples of arene-analogues with oxygen remain seldom. Chi, Zeng and their coworkers separately reported bis(anthraoxa) quinodimethanes with nine and ten fused six-membered rings and oxygen-embedded quinoidal pentacene and nonacene as arene-analogues with formal pyran units.[4] Extended O-doped polycyclic aromatic hydrocarbons and molecular ribbons have been synthesized by Bonifazi and coworkers.[5] You and coworkers have recently devised a [4 + 2] synthetic strategy[6] to synthesize O-containing porphyrins and investigated their absorption and electrochemical properties.[7] Formal pyran units have also been incorporated into conjugated molecules with radical character.[8] In fact, conjugated molecules incorporating oxygen atoms in their backbones have been investigated less for organic electronic materials comparing with their sulfur and nitrogen atom counterparts.[9] In this regard, the series of studies

by Bnedikov and coworkers have aroused interest in oligofurans[10] which possess many of the properties which enable them to be interesting as organic electronic materials.[10,11] Nakamura and coworkers devised a new synthetic method for polycyclic furans and investigated their emissive and semiconducting properties in the solid state,[12] demonstrating the high potential of fused polycyclic furans as organic optoelectronic materials.[9,12,13]
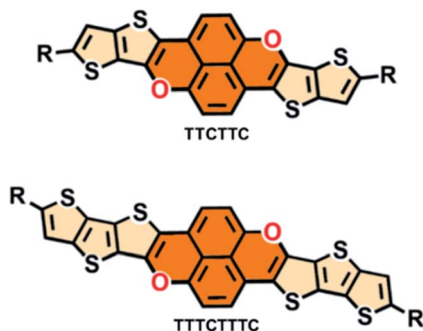
Considering the fact that thiophene, in particular fused-thiophene rings containing fused conjugated molecules such as **BTBT** and its analogues,[14] show outstanding semiconducting properties, it is interesting to integrate a pyran moiety with fused-thiophene rings to form newly fused conjugated molecules as potential organic electronic materials. In this paper, we report two highly fused conjugated molecules, thieno[2″,3″:4′,5′] thieno[3′,2′:2,3] chromeno [6,5,4-*def*] thieno[2′,3′:4,5] thieno[3,2-*b*] chromene (**TTCTTC**) and thieno[2‴,3‴:4′,5″] thieno[2″,3″:4′,5″] thieno [3′,2′:2,3] chromeno[6, 5,4-*def*] thieno[2″,3″:4′,5′] thieno[2′,3′:4,5] thieno[3,2-*b*] chromene (**TTTCTTTC**) (Scheme 1), with two formal pyran units. Two alkyl chains are attached to both **TTCTTC** (R = *n*-octadecyl) and **TTTCTTTC** (R = 2-ethylhexyl) to ensure their good solubility in organic solvents. Both **TTCTTC** and **TTTCTTTC** can be synthesized in 3 steps with acceptable yields. The results reveal that they have high HOMO energy levels, up to −4.69 eV. Thin films of these two compounds exhibit p-type semiconducting properties with hole mobility up to 0.39 cm^2 V^{-1} s^{-1}. In particular, the thin film of **TTCTTC** is emissive with a quantum yield of 16.5% in the solid state.

[a]Beijing National Laboratory for Molecular Sciences, CAS Key Laboratory of Organic Solids, CAS Center of Excellence of Molecular Sciences, Institute of Chemistry, Chinese Academy of Sciences, Beijing, 100190, P. R. China

[b]University of Chinese Academy of Sciences, Beijing 100049, P. R. China

Scheme 1 Chemical structures of TTCTTC and TTTCTTTC.

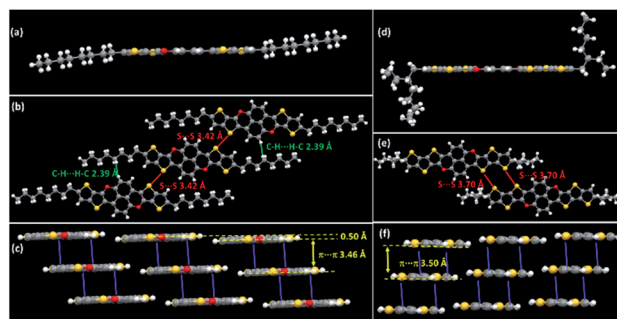Fig. 1 Molecular structures and intermolecular interactions and arrangements of TTCTTC (a–c) and TTTCTTTC (d–f) crystal lattices.

Results and discussion

The synthetic approaches are outlined in Scheme 2. The synthesis started with compound **1** which underwent a halogen–lithium exchange reaction to afford zinc reagent **2**. The selective Negishi coupling of **2** with 3-bromo-2-iodothieno[3,2-*b*]thiophene and 3-bromo-2-iododithieno[3,2-*b*:2′,3′-*d*]thiophene in the presence of PdCl$_2$(PPh$_3$)$_2$ yielded **3a** and **4a** in 49.8% and 52.3% yields, respectively. The respective demethylation of **3a** and **4a** by BBr$_3$ afforded **3b** and **4b**. The intramolecular C–O coupling reaction within **3b** and **4b**, which was catalyzed by CuI/1,10-phenloine, yielded the target molecules **TTCTTC** and **TTTCTTTC** in 61.5% and 58.3% yields, respectively. The chemical structures of **TTCTTC** and **TTTCTTTC** were characterized with NMR spectra and MS data, and their purities were checked with elemental analysis (see ESI†). Thermal decomposition was not observed for **TTCTTC** and **TTTCTTTC** when the temperatures were below 282 °C and 316 °C, respectively, based on the thermogravimetric analysis data (see Fig. S1†).

Single crystals of **TTCTTC** and **TTTCTTTC** suitable for X-ray analysis were obtained by crystallization from the respective solutions in toluene, and their crystal structures were successfully determined (see ESI†). Fig. 1 shows their molecular structures and intermolecular arrangements. Obviously, the

conjugated cores of both **TTCTTC** and **TTTCTTTC** are fully planar. All bond lengths (see Tables S2 and S3†) are in the normal ranges. Molecules of **TTCTTC** interact to form layers *via* short interatomic contacts (C···H short contacts, 2.39 Å; S···S short contacts, 3.42 Å). The molecular layers are further assembled to form columns *via* π–π interactions (3.46 Å). For **TTTCTTTC**, molecules interact to form layers *via* interatomic S···S contacts (3.70 Å), and the conjugated cores are further assembled by intermolecular π–π interactions (3.50 Å) as depicted in Fig. 1. Such intermolecular interactions and arrangements are beneficial for intermolecular charge transport as discussed below.

The cyclic voltammograms of **TTCTTC** and **TTTCTTTC** were measured and are shown in Fig. 2. As shown in Fig. 2, two reversible oxidation waves were detected at $E_{ox1}^{1/2} = -0.01$ V (*vs.* Fc/Fc$^+$) and $E_{ox2}^{1/2} = 0.41$ V (*vs.* Fc/Fc$^+$) for **TTCTTC**, whereas **TTTCTTTC** displayed two oxidation waves at $E_{ox1}^{1/2} = 0.02$ V (*vs.* Fc/Fc$^+$) and $E_{ox2}^{1/2} = 0.41$ V (*vs.* Fc/Fc$^+$). Based on the respective onset oxidation potentials, HOMO energies were estimated to be −4.69 eV for **TTCTTC** and −4.71 eV for **TTTCTTTC**. As discussed below, the optical band gaps (E_g^{opt}) of **TTTCTTTC** and

Scheme 2 The synthesis of TTCTTC and TTTCTTTC.
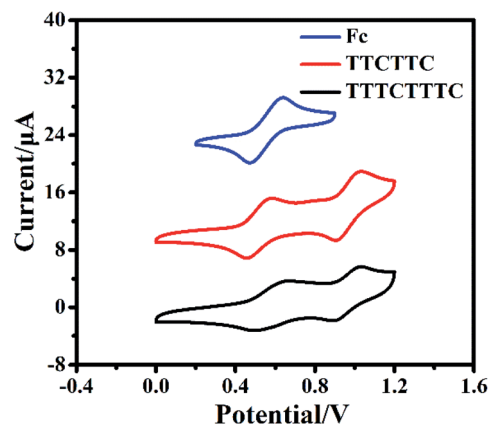
Fig. 2 Cyclic voltammograms of TTCTTC (0.1 mM) and TTTCTTTC (0.1 mM) in *o*-dichlorobenzene at a scan rate of 100 mV s^{-1}, with Pt as the working and counter electrodes, and Ag/AgCl (saturated KCl) as the reference electrode, and *n*-Bu$_4$NPF$_6$ (0.1 M) as the supporting electrolyte. The cyclic voltammogram of ferrocene was measured under the same conditions.

TTCTTC were estimated to be 2.58 eV and 2.48 eV, respectively. Accordingly, the LUMO energies of **TTCTTC** and **TTTCTTTC** were calculated to be −2.11 eV and −2.23 eV, respectively, using the equation: LUMO = HOMO + E_g^{opt}. On the basis of the high lying HOMO energy levels, which are comparable with those of TTF[15] and pentacene,[16] thin films of **TTCTTC** and **TTTCTTTC** are expected to show p-type semiconducting behavior. The high HOMO energy levels are also supported by the DFT calculations. Fig. S5† shows the calculated HOMO and LUMO orbitals of **TTCTTC** and **TTTCTTTC**. It is clear that the HOMO orbitals are mainly distributed on the central chromeno[6,5,4-*def*]chromene cores for both molecules, while their LUMO orbitals are evenly distributed across the whole conjugated backbone. Therefore, the resultant excited states of the two molecules exhibit charge transfer features from the central conjugated core to the fused-thiophenes. The calculated HOMO energies of **TTCTTC** and **TTTCTTTC** were −4.45 eV and −4.48 eV, whereas the respective calculated LUMO energies were −1.34 eV and −1.54 eV. The calculated HOMO energies of **TTCTTC** and **TTTCTTTC** are close as determined with cyclic voltammetry as discussed above.

Fig. 3 shows the absorption spectra of **TTCTTC** and **TTTCTTTC** in solution and solid state. The solution of **TTCTTC** shows strong absorption at 295 nm, 406 nm, 436 nm, and 463 nm. In comparison, the absorption peaks of **TTTCTTTC** in solution are red-shifted to 319 nm, 334 nm, 422 nm, 450 nm, and 478 nm. Such absorption red-shift can be attributed to the elongation of conjugation length of **TTTCTTTC** compared with **TTCTTC**. This agrees with the calculated electron absorptions based on their optimized geometries. As shown in Table S4,† the calculated absorption peaks are at 461.1 nm ($S_0 \rightarrow S_2$) and 313.8 nm ($S_0 \rightarrow S_6$) for **TTCTTC** in solution and those for **TTTCTTTC** are at 490.9 nm ($S_0 \rightarrow S_2$) and 349.3 nm ($S_0 \rightarrow S_4$). These are in good agreement with the respective two dominant absorption bands of **TTCTTC** and **TTTCTTTC**. The other absorption peaks may be caused by electron-vibration coupling, which is usually observed for planar conjugated molecules.

The absorption spectra of both molecules are red-shifted in their solid states compared with the respective absorption in solution (see Fig. 3). For instance, the solid sample of **TTCTTC** shows absorption at 301 nm, 420 nm, 450 nm and 482 nm which are red-shifted by 6 nm, 14 nm, 14 nm and 19 nm, respectively, in comparison with those in solution. On the basis of the respective onset absorption in the solid state, the optical bandgaps of **TTCTTC** and **TTTCTTTC** were estimated to be 2.33 eV and 2.31 eV, respectively.

The emission spectra in solution and solid state were measured (see Fig. S6†) and their emission maxima, quantum yields and fluorescence lifetimes are listed in Table S5.† To our delight, both solutions of **TTCTTC** and **TTTCTTTC** are emissive with quantum yields of 13.8% and 13.6%, respectively. Furthermore, **TTCTTC** is also emissive around 571 nm in the solid state with a quantum yield of 16.5%, while **TTTCTTTC** shows rather weak emission in the solid state (Table S5 and Fig. S7†).

Considering that **TTCTTC** and **TTTCTTTC** possess high HOMO energy levels, we investigated their absorption spectra after oxidation. It was reported that electron donors with high HOMO energy levels such as N–N linked bicarbazole or biacridine derivatives,[17] and tetrabenzoporphyrin,[18] can be oxidized by acids such CF_3COOH. As shown in Fig. 4, new absorption peaks around 650 nm and 980 nm were observed after the addition of CF_3COOH (1% wt) into the CH_2Cl_2 solution of **TTCTTC**. Similarly, new absorption peaks around 680 nm and 1150 nm emerged after the addition of CF_3COOH (1% wt) into the CH_2Cl_2 solution of **TTTCTTTC**. Furthermore, strong ESR signals with g = 2.0039 and 2.0040 were observed for both solutions of **TTCTTC** and **TTTCTTTC** after addition of CF_3-COOH, respectively (see Fig. S8†). We also measured the absorption spectra of **TTCTTC** and **TTTCTTTC** (see Fig. S9†) after electrochemical oxidation by applying oxidation potentials at 0.6 V (*vs.* Ag/AgCl). Clearly, the absorption after addition of CF_3COOH matches well with the respective ones after electrochemical oxidation. These results show that both **TTCTTC** and **TTTCTTTC** can be oxidized by CF_3COOH. This could be attributed to their high HOMO energy levels.

In order to evaluate the charge transporting properties, organic field-effect transistor (OFET) devices with bottom-gate/bottom-contact (BGBC) structures were fabricated by vacuum
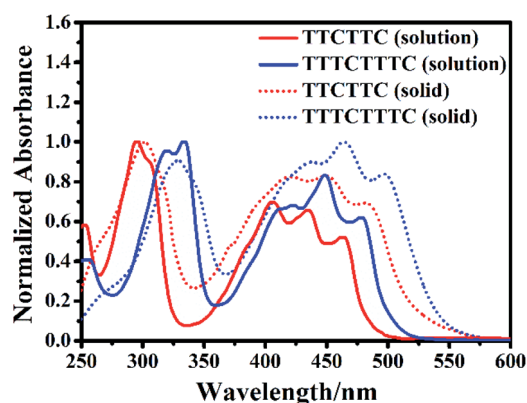

Fig. 3 Normalized UV-vis absorption spectra of the dichloromethane (10 μM) solutions of **TTCTTC** and **TTTCTTTC** and their solid samples.
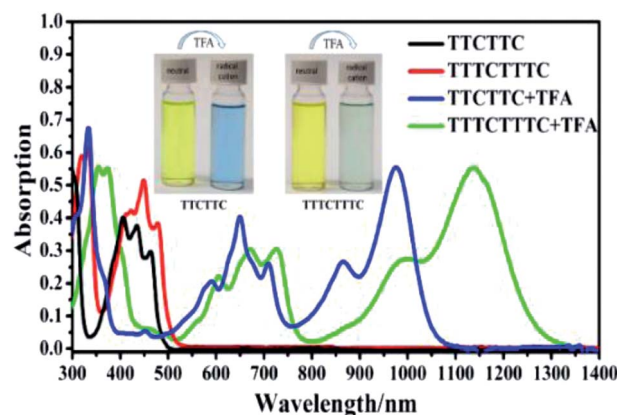

Fig. 4 UV-vis-NIR absorption spectra of CH_2Cl_2 solutions (10 μM) of **TTCTTC** and **TTTCTTTC** and related UV-vis-NIR absorption spectra after the addition of CF_3COOH (1% wt).
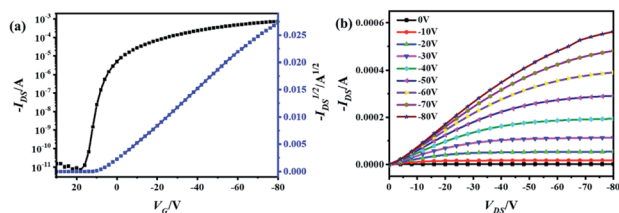
Fig. 5 Transfer (a) and output (b) characteristics of OFETs with thin films of **TTCTTC** deposited on OTS-modified SiO₂/Si substrate.

deposition of the thin films on the octadecyltrichlorosilane (OTS)-modified SiO₂ (300 nm)/Si substrates with a pre-patterned gold source and drain electrodes. The devices were measured under an inert atmosphere. Fig. 5, S10 and S11† show the transfer and output curves, from which the semiconducting performance data was extracted and summarized in Table S6.† In the transfer curves for OFETs with thin films of **TTCTTC** and **TTTCTTTC**, I_{DS} increases by applying the negative V_{GS} (see Fig. 5, S10 and S11†). Thus, both thin-films exhibit p-type semiconducting behavior. This is in good agreement with the high HOMO energy levels of **TTCTTC** and **TTTCTTTC** as discussed above. The maxima and average hole mobilities of devices with thin films of **TTCTTC** deposited on the substrates at 25 °C were measured to be 0.31 and 0.19 cm² V⁻¹ s⁻¹, respectively, with high $I_{on/off}$ ratios. The average hole mobility for a thin film of **TTCTTC** slightly increased to 0.25 cm² V⁻¹ s⁻¹ by increasing the substrate temperature to 50 °C. But, the hole mobility started to decrease by further increasing the substrate temperature to 90 °C as listed in Table S6.† In comparison, the maxima hole mobility is only 0.016 cm² V⁻¹ s⁻¹ for the thin film of **TTTCTTTC** deposited on the substrate at 25 °C (see Table S6†). Only a small enhancement of charge mobility was observed by increasing the substrate temperature for the thin film of **TTTCTTTC**. This can be attributed to the poor crystallinity of the thin film of **TTTCTTTC** (Fig. S12–S14†). The intermolecular transfer integrals were calculated on the basis of the crystal structures of **TTCTTC** and **TTTCTTTC**. As shown in Fig. S4,† **TTCTTC** shows multiple charge transfer pathways with transfer integrals of 25.97 and −36.19 meV, which are larger than those of **TTTCTTTC** (14.34 meV and 1.35 meV). This is in good agreement with the observation that the thin film of **TTCTTC** exhibits higher hole mobility than that of **TTTCTTTC**.

Conclusions

In conclusion, we report the synthesis, characterization and semiconducting properties of two fused conjugated molecules, **TTCTTC** and **TTTCTTTC**, entailing pyran and fused thiophene moieties. The crystal structures show that molecules of **TTCTTC** interact *via* C···H and S···S interactions to form layers which are further connected *via* π–π stacking with a distance of 3.46 Å. Intermolecular π–π interactions were also observed for **TTTCTTTC** in the crystal lattice. Both electrochemical measurements and DFT calculations show that both **TTCTTC** and **TTTCTTTC** possess high HOMO energy levels. As a result,

they can be oxidized to their radical cations by CF₃COOH. The resulting radical cations show strong absorption in the near-infrared light region up to 1300 nm. Both conjugated molecules are emissive in solution, with fluorescence quantum yields up to 13.8%. But, only **TTCTTC** shows relatively strong emission in the solid state. Both thin films of **TTCTTC** and **TTTCTTTC** exhibit p-type semiconducting properties. The thin film of **TTCTTC** shows relatively high hole mobility of up to 0.39 cm² V⁻¹ s⁻¹, whereas the average hole mobility of a thin film of **TTTCTTTC** is only 0.017 cm² V⁻¹ s⁻¹. This can be attributed to the fact that the thin film of **TTCTTC** shows high crystallinity based on the XRD studies, while the thin film of **TTTCTTTC** is of low crystallinity. Further elongation of the conjugation lengths and incorporation of functional groups to these fused and expanded conjugated molecules are underway.

Experimental section

Synthesis of 3a

Under a nitrogen atmosphere, 2.7 ml of *n*-butyl lithium (1.6 M) was added to **1** (0.67 g, 1.95 mmol) in dry THF solution (20 ml) at −78 °C. The resulting solution was stirred at this temperature for 10 min. When the reaction system was slowly warmed up to 0 °C, 2.5 ml of ZnCl₂ (2 M) in dry THF was added to the system. After the reaction mixture was stirred for 30 min at 0 °C, 3-bromo-2-iodo-5-octylthieno[3,2-*b*]thiophene[19] (3.0 g, 6.6 mmol) and PdCl₂(PPh₃)₂ (50 mg, 0.07 mmol) were added. The reaction system was then heated to 70 °C and stirred for 12 h under a nitrogen atmosphere. After removal of the THF, 50 ml of water was added to the mixture which was then extracted with dichloromethane and dried over Na₂SO₄. After removal of dichloromethane, the crude product was purified using silica gel column chromatography with petroleum ether (60–90 °C)/dichloromethane (2 : 1, v/v) to give **3a** (820 mg, 0.97 mmol) in 49.8% yield. ¹H NMR (300 MHz, CDCl₃, 25 °C) δ = 7.42 (d, J = 9 Hz, 2H), 7.00 (s, 2H), 6.88 (d, J = 9 Hz, 2H), 3.62 (s, 6H), 2.92 (t, J = 7.5 Hz, 4H), 1.75 (d, J = 6 Hz, 4H), 1.43–1.30 (m, 20H), 0.90 (t, J = 6 Hz, 6H). ¹³C NMR (75 MHz, CDCl₃, 25 °C) δ = 157.22, 146.87, 141.62, 137.70, 135.02, 132.02, 125.95, 121.03, 117.00, 105.89, 101.55, 56.14, 31.90, 31.67, 31.22, 29.38, 29.26, 29.14, 22.71, 14.15. HRMS (MALDI-TOF): *m/z* calcd for C₄₀H₄₆Br₂O₂S₄: 844.0747 [M]⁺; found: 844.0758.

Synthesis of 3b

Under a nitrogen atmosphere, **3a** (265 mg, 0.31 mmol) was dissolved in 20 ml of dry dichloromethane. The solution was cooled to −78 °C, and 1 ml of BBr₃ (1 M) solution in dichloromethane was added slowly. Then, it was allowed to increase to room temperature and stirred for 12 h. 50 ml of water was added to the mixture which was then extracted with dichloromethane and dried over Na₂SO₄. After removal of dichloromethane, the mixture was purified using silica gel column chromatography with petroleum ether (60–90 °C)/dichloromethane (1 : 1, v/v) to give **3b** (188 mg, 0.23 mmol) in 74.2% yield. ¹H NMR (400 MHz, [D₈]THF, 25 °C) δ = 8.75 (s, 2H), 7.26 (d, J = 8 Hz, 2H), 7.11 (s, 2H), 6.77 (d, J = 8 Hz, 2H), 2.97 (t,

J = 8 Hz, 4H), 1.86–1.73 (m, 4H), 1.58–1.24 (m, 20H), 0.95 (t, J = 6 Hz, 6H). ^{13}C NMR (100 MHz, [D$_8$]THF, 25 °C) δ = 155.28, 146.15, 142.04, 137.64, 135.37, 131.14, 125.50, 119.82, 117.12, 109.47, 101.78, 31.87, 31.73, 30.78, 29.34, 29.25, 28.98, 22.57, 13.46. HRMS (ESI): m/z calcd for C$_{38}$H$_{42}$Br$_2$O$_2$S$_4$ + Br$^-$: 898.9576 [M + Br]$^-$; found: 898.9583.

Synthesis of TTCTTC

3b (106 mg, 0.13 mmol) and K$_2$CO$_3$ (300 mg, 2.17 mmol) were added to 30 ml of dry toluene in a Schlenk tube. After nitrogen gas was bubbled through the mixture for 10 min, 1,10-phenanthroline (20 mg, 0.11 mmol) and CuI (10 mg, 0.05 mmol) was added under a nitrogen atmosphere. It was then heated to 100 °C and stirred for 24 h. Then, after cooling to room temperature, the reaction mixture was directly subjected to separation using basic Al$_2$O$_3$ column chromatography with toluene as the eluent to give **TTCTTC** (52 mg) in 61.5% yield. ^{1}H NMR (400 MHz, [D$_8$]THF/CS$_2$ v/v = 1 : 4, 25 °C) δ = 6.80 (s, 2H), 6.53 (d, J = 8.0 Hz, 2H), 6.50 (d, J = 8.0 Hz, 2H), 2.83 (t, J = 7.6 Hz, 4H), 1.35–1.22 (m, 24H), 0.86 (m, 6H). ^{13}C NMR (100 MHz, [D$_8$]THF/CS$_2$ v/v = 1 : 4, 25 °C) δ = 150.28, 149.01, 143.45, 135.36, 126.69, 123.50, 121.78, 117.32, 117.01, 114.30, 110.02, 32.32, 31.92, 31.45, 29.83, 29.75, 29.58, 23.27, 14.45. HRMS (MALDI-TOF) m/z calcd for C$_{38}$H$_{40}$O$_2$S$_4$: 656.1911 [M]$^+$; found 656.1892; elemental analysis calcd (%) for C$_{38}$H$_{40}$O$_2$S$_4$: C, 69.47; H, 6.14; S, 19.52; found: C 69.74; H 6.09; S 19.37.

Synthesis of 4a

Under a nitrogen atmosphere, 3.0 ml of n-butyl lithium (1.6 M) was added to **1** (0.74 g, 2.14 mmol) in dry THF solution (20 ml) at −78 °C. The resulting solution was stirred at this temperature for another 10 min. Then, the reaction system was warmed to 0 °C, and 3.5 ml ZnCl$_2$ (2 M) in THF was added slowly. The reaction was stirred at this temperature for 30 min, then 3-bromo-6-(2-ethylhexyl)-2-iododithieno[3,2-b:2′,3′-d]thiophene^{19} (3.0 g, 5.85 mmol) and PdCl$_2$(PPh$_3$)$_2$ (30 mg, 0.04 mmol) were added to the reaction system. The reaction was heated to 70 °C and stirred at this temperature for 12 h. Then, the mixture was cooled and evaporated to remove the excess THF. 50 ml of water was added to the mixture which was then extracted with dichloromethane and dried over Na$_2$SO$_4$. After removal of dichloromethane, the crude product was purified using silica gel column chromatography with petroleum ether (60–90 °C)/dichloromethane (2 : 1, v/v) to give **4a** (1.08 g) in 52.3% yield. ^{1}H NMR (400 MHz, CDCl$_3$, 25 °C) δ = 7.46 (d, J = 8.0 Hz, 2H), 7.03 (s, 2H), 6.91 (d, J = 8 Hz, 2H), 3.64 (s, 6H), 2.87 (d, J = 4 Hz, 4H), 1.67 (m, 2H), 1.50–1.24 (m, 16H), 0.95–0.91 (m, 12H). ^{13}C NMR (100 MHz, CDCl$_3$, 25 °C) δ = 157.31, 146.01, 141.13, 138.67, 132.24, 129.67, 128.09, 125.93, 120.77, 118.57, 105.91, 105.87, 102.60, 56.15, 41.54, 35.22, 32.44, 28.94, 25.55, 23.05, 14.20, 10.89. HRMS (MALDI-TOF) m/z calcd for C$_{44}$H$_{46}$O$_2$S$_6$: 956.0188 [M]$^+$; found 956.0120.

Synthesis of 4b

Under a nitrogen atmosphere **4a** (420 mg, 0.44 mmol) was dissolved in 20 ml of dry dichloromethane. The mixture was then cooled to −78 °C, and 1 ml of BBr$_3$ (1 M) solution in dichloromethane was added slowly at this temperature. Then, it was allowed to increase to room temperature and stirred for 12 h. 50 ml of water was added to the mixture which was then extracted with dichloromethane and dried over Na$_2$SO$_4$. After removal of the solvents, the crude product was purified using silica gel column chromatography with petroleum ether (60–90 °C)/dichloromethane (1 : 1, v/v) to give **4b** (294 mg) in 72.7% yield. ^{1}H NMR (400 MHz, [D$_8$]THF, 25 °C) δ = 7.17 (d, J = 8 Hz, 2H), 7.02 (s, 2H), 6.67 (d, J = 8 Hz, 2H), 2.79 (d, J = 8 Hz, 4H), 1.57 (m, 2H), 1.31–1.23 (m, 16H), 0.85–0.79 (m, 12H). ^{13}C NMR (125 MHz, [D$_8$]THF, 25 °C) δ = 155.48, 145.52, 141.77, 140.25, 138.56, 131.39, 129.55, 128.01, 125.56, 119.52, 118.81, 109.60, 102.23, 41.65, 34.83, 32.38, 28.84, 25.47, 22.90, 13.47, 10.21. HRMS (ESI) m/z calcd for C$_{42}$H$_{42}$Br$_2$O$_4$S$_6$ + Br$^-$: 1010.9018 [M + Br]$^-$; found 1010.9071.

Synthesis of TTTCTTTC

4b (114 mg, 0.12 mmol), K$_2$CO$_3$ (300 mg, 2.17 mmol) and 60 ml of toluene were added to a Schlenk tube. After nitrogen gas was bubbled through the solution for 10 min, CuI (10 mg, 0.05 mmol) and 1,10-phenanthroline (20 mg, 0.11 mmol) were added. The reaction mixture was heated to 100 °C and stirred for 24 h. Then, the reaction mixture was separated directly using basic Al$_2$O$_3$ column chromatography using toluene as the eluent to give **TTTCTTTC** (51 mg) in 58.3% yield as a yellow solid. ^{1}H NMR (400 MHz, [D$_8$]THF/CS$_2$ v/v = 1 : 4, 25 °C) δ = 6.91 (s, 2H), 6.60 (d, J = 8 Hz, 2H), 6.56 (d, J = 8 Hz, 2H), 2.81 (d, J = 8 Hz, 4H), 1.62 (m, 2H), 1.37–1.22 (m, 16H), 0.92–0.88 (m, 12H). ^{13}C NMR (100 MHz, [D$_8$]THF/CS$_2$ v/v = 1 : 4, 25 °C) δ = 150.26, 147.11, 143.89, 141.05, 129.58, 129.15, 127.67, 123.44, 121.51, 118.77, 116.69, 114.36, 110.12, 41.73, 35.36, 32.73, 29.23, 25.94, 23.52, 14.34, 10.97. HRMS (MALDI-TOF) m/z calcd for C$_{42}$H$_{40}$O$_2$S$_6$: 768.1352 [M]$^+$; found 768.1348; elemental analysis calcd (%) for C$_{42}$H$_{40}$O$_2$S$_6$: C, 65.59; H, 5.24; S, 25.01; found: C 65.38; H 5.21; S 24.98.

Fabrication of OFET devices

OFET devices for **TTCTTC** and **TTTCTTTC** were fabricated in a BGBC configuration. A layer of 300 nm thick SiO$_2$ was used as a gate dielectric layer and a heavily doped n-type silicon wafer was chosen as the gate electrode. The gold drain/source (D/S) electrodes with thickness of 30 nm were adopted and deposited on the substrates by photo-lithography. Mixed solutions of hydrogen peroxide and sulfuric acid were used to treat the substrates and were soaked for about 0.5 h. Then they were cleaned using deionized water and rinsed in isopropanol. The obtained Si/SiO$_2$ substrates were then put into a vacuum oven and treated with OTS at 125 °C for 4 h. The OTS modified substrates were then washed with chloroform, n-hexane and isopropanol, respectively. Molecules of **TTCTTC** and **TTTCTTTC** were slowly deposited (0.1 Å s^{-1}) onto the OTS modified substrates to form the thin films (about 40 nm in thickness) at different substrate temperatures (25, 50, and 90 °C). The measurements were conducted under a nitrogen atmosphere using a Keithley 4200 SCS analyzer. The mobilities were

calculated with the equation: $I_D = \mu C_i (W/2L)(V_G - V_{th})^2$, in which I_D is the drain current, C_i is capacitance per unit area of the insulating layer (11.5 nF cm^{-2}), W is channel width, L is channel length, and V_{th} is the threshold voltage.

Conflicts of interest

There are no conflicts to declare.

Acknowledgements

References

1 M. Stępień, E. Gońka, M. Żyła and N. Sprutta, *Chem. Rev.*, 2017, **117**, 3479; X.-Y. Wang, X. Yao, A. Narita and K. Müllen, *Acc. Chem. Res.*, 2019, **52**, 2491; M. E. Cinar and T. Ozturk, *Chem. Rev.*, 2015, **115**, 3036; M. Hirai, N. Tanaka, M. Sakai and S. Yamaguchi, *Chem. Rev.*, 2019, **119**, 8291; L. Qiu, C. Yu, N. Zhao, W. Chen, Y. Guo, X. Wan, R. Yang and Y. Liu, *Chem. Commun.*, 2012, **48**, 12225; S. C. Rasmussen, S. J. Evenson and C. B. McCausland, *Chem. Commun.*, 2015, **51**, 4528; H. Yamada, Y. Yamaguchi, R. Katoh, T. Motoyama, T. Aotake, D. Kuzuhara, M. Suzuki, T. Okujima, H. Uno, N. Aratani and K.-i. Nakayama, *Chem. Commun.*, 2013, **49**, 11638.

2 T. Zheng, Z. Cai, R. Ho-Wu, S. H. Yau, V. Shaparov, T. Goodson and L. Yu, *J. Am. Chem. Soc.*, 2016, **138**, 868; Y. Huang, D. Wu, J. Huang, Q. Guo, J. Li and J. You, *Angew. Chem., Int. Ed.*, 2014, **53**, 12158; S.-L. Suraru and F. Würthner, *Angew. Chem., Int. Ed.*, 2014, **53**, 7428; S. C. Rasmussen, R. L. Schwiderski and M. E. Mulholland, *Chem. Commun.*, 2011, **47**, 11394; H. J. Son, F. He, B. Carsten and L. Yu, *J. Mater. Chem.*, 2011, **21**, 18934; J. Cao, C. Zuo, B. Du, X. Qiu and L. Ding, *Chem. Commun.*, 2015, **51**, 12122.

3 H. Dong, C. Wang and W. Hu, *Chem. Commun.*, 2010, **46**, 5211; H. Yao, L. Ye, H. Zhang, S. Li, S. Zhang and J. Hou, *Chem. Rev.*, 2016, **116**, 7397; S. Vegiraju, D.-Y. Huang, P. Priyanka, Y.-S. Li, X.-L. Luo, S.-H. Hong, J.-S. Ni, S.-H. Tung, C.-L. Wang, W.-C. Lien, S. L. Yau, C.-L. Liu and M.-C. Chen, *Chem. Commun.*, 2017, **53**, 5898; D. Wang, X. Qiao, G. Ouyang, H. Wu and H. Li, *Chem. Commun.*, 2019, **55**, 6253; M. Melucci, M. Zambianchi, L. Favaretto, M. Gazzano, A. Zanelli, M. Monari, R. Capelli, S. Troisi, S. Toffanin and M. Muccini, *Chem. Commun.*, 2011, **47**, 11840; X. Shi, J. Chang and C. Chi, *Chem. Commun.*, 2013, **49**, 7135.

4 S. Dong, T. Y. Gopalakrishna, Y. Han, H. Phan, T. Tao, Y. Ni, G. Liu and C. Chi, *J. Am. Chem. Soc.*, 2019, **141**, 62; Y. Wang, S. Qiu, S. Xie, L. Zhou, Y. Hong, J. Chang, J. Wu and Z. Zeng, *J. Am. Chem. Soc.*, 2019, **141**, 2169.

5 A. Berezin, N. Biot, T. Battisti and D. Bonifazi, *Angew. Chem., Int. Ed.*, 2018, **57**, 8942; S. Daphné, D. Nicola and B. Davide, *Angew. Chem., Int. Ed.*, 2016, **55**, 5947.

6 J. Yin, M. Tan, D. Wu, R. Jiang, C. Li and J. You, *Angew. Chem., Int. Ed.*, 2017, **56**, 13094.

7 C. Li, L. Zhu, W. Liang, R. Su, J. Yin, Y. Hu, Y. Lan, D. Wu and J. You, *Chem. Sci.*, 2019, **10**, 7274.

8 K. P. Rao, T. Kusamoto, F. Toshimitsu, K. Inayoshi, S. Kume, R. Sakamoto and H. Nishihara, *J. Am. Chem. Soc.*, 2010, **132**, 12472; C. M. Wehrmann, R. T. Charlton and M. S. Chen, *J. Am. Chem. Soc.*, 2019, **141**, 3240; O. Anamimoghadam, M. D. Symes, D.-L. Long, S. Sproules, L. Cronin and G. Bucher, *J. Am. Chem. Soc.*, 2015, **137**, 14944.

9 Z. Zhao, H. Nie, C. Ge, Y. Cai, Y. Xiong, J. Qi, W. Wu, R. T. K. Kwok, X. Gao, A. Qin, J. W. Y. Lam and B. Z. Tang, *Adv. Sci.*, 2017, **4**, 1700005; H. Tsuji and E. Nakamura, *Acc. Chem. Res.*, 2017, **50**, 396.

10 O. Gidron and M. Bendikov, *Angew. Chem., Int. Ed.*, 2014, **53**, 2546.

11 Y. Xiong, J. Tao, R. Wang, X. Qiao, X. Yang, D. Wang, H. Wu and H. Li, *Adv. Mater.*, 2016, **28**, 5949.

12 C. Mitsui, J. Soeda, K. Miwa, H. Tsuji, J. Takeya and E. Nakamura, *J. Am. Chem. Soc.*, 2012, **134**, 5448; H. Tsuji, C. Mitsui, L. Ilies, Y. Sato and E. Nakamura, *J. Am. Chem. Soc.*, 2007, **129**, 11902.

13 D. Chen, J. Li, W. Ma, B. Li, Y. Zhen, X. Zhu, W. Hu, H. Tsuji and E. Nakamura, *Asian J. Org. Chem.*, 2018, **7**, 2228; K. Nakanishi, D. Fukatsu, K. Takaishi, T. Tsuji, K. Uenaka, K. Kuramochi, T. Kawabata and K. Tsubaki, *J. Am. Chem. Soc.*, 2014, **136**, 7101.

14 T. Mori, T. Nishimura, T. Yamamoto, I. Doi, E. Miyazaki, I. Osaka and K. Takimiya, *J. Am. Chem. Soc.*, 2013, **135**, 13900; K. Niimi, S. Shinamura, I. Osaka, E. Miyazaki and K. Takimiya, *J. Am. Chem. Soc.*, 2011, **133**, 8732.

15 S. Adeel, M. E. Abdelhamid, A. Nafady, Q. Li, L. L. Martin and A. M. Bond, *RSC Adv.*, 2015, **5**, 18384.

16 O. L. Griffith, J. E. Anthony, A. G. Jones and D. L. Lichtenberger, *J. Am. Chem. Soc.*, 2010, **132**, 580.

17 P. Pandit, K. Yamamoto, T. Nakamura, K. Nishimura, Y. Kurashige, T. Yanai, G. Nakamura, S. Masaoka, K. Furukawa, Y. Yakiyama, M. Kawano and S. Higashibayashi, *Chem. Sci.*, 2015, **6**, 4160.

18 Y. Zhen, K. Inoue, Z. Wang, T. Kusamoto, K. Nakabayashi, S.-i. Ohkoshi, W. Hu, Y. Guo, K. Harano and E. Nakamura, *J. Am. Chem. Soc.*, 2018, **140**, 62.

19 H.-Y. Chen, G. Schweicher, M. Planells, S. M. Ryno, K. Broch, A. J. P. White, D. Simatos, M. Little, C. Jellett, S. J. Cryer, A. Marks, M. Hurhangee, J.-L. Brédas, H. Sirringhaus and I. McCulloch, *Chem. Mater.*, 2018, **30**, 7587.